



Modelling Aircraft Noise near Airports

André S. Sousa¹, João M. G. S Oliveira², António J. N. M. Aguiar³

¹G Air Training Centre, Portugal
andre.sousa@gairg.com

²IDMEC, Instituto Superior Técnico, Universidade de Lisboa, Lisboa, Portugal
joliveira@tecnico.ulisboa.pt

³TAP Portugal, Lisboa, Portugal
aaguiar@tap.pt

Abstract

We have developed, implemented and validated a model for aircraft noise prediction near airports. The aircraft as a noise source, including noise directivity, is determined from the NPD (Noise Power Distance) data in the Aircraft Noise and Performance database, provided by the Eurocontrol. For the atmospheric sound propagation a hybrid model was used, based on the approach specified in the Imagine project. For elevation angles of the aircraft relative to the observer on the ground above 50°, a 2-ray model is used. For lower elevation angles, below 40°, a Green Function Parabolic Equation method is used. For elevation angles between 40° and 50° a linear interpolation is used.

Comparison with experimental results from an approach of an A320 at Lisbon Airport shows that the model correctly predicts the Sound Exposure Level (SEL) and the SEL spectrum. We were also able to use the experimental data from two noise monitoring stations (located at Camarate and at the Airport) for a real departure procedure of an A320 at Lisbon Airport. The measured and calculated SEL differ by 0.3 dB at Camarate station and 1.4 dB at the airport station. The maximum SPL differ by 0.6 dB at Camarate station and 4.0 dB at the airport stations. These results show that the model that was developed can be used with some confidence to predict noise level from aircraft in the vicinity of airports. It can also be used to optimize trajectories to reduce noise at one or any number of ground stations.

Keywords: Airport noise, atmospheric propagation, hybrid model.

PACS no. 43.28.Js, 43.50.Lj

1 Introduction

For communities established in the vicinity of airports, aviation noise has become a major concern as the regular operation of multiple aircraft can become an unwelcome presence.

Following the directives of aviation authorities, several computational applications have been developed by national regulators in order to predict noise contours in major airports that can help to minimize the impact of aviation noise by providing tools that facilitate land use management and that offer a direct approach to mitigate noise impact in specific areas. These computational applications often use engineering models, but in some cases more accurate prediction models are useful. For the propagation of sound in the atmosphere, using two accepted propagation models, the Green's Function Parabolic Equation (GFPE) method and the ray model, we developed a hybrid propagation model in



Matlab. This algorithm is combined with the definition of aircraft as complex noise sources by applying a reverse engineering process to published Noise-Power-Distance (NPD) experimental data. This program is well suited for noise prediction in airports as it is capable of translating in-flight parameters to quantities relevant for the noise propagation algorithms.

2 The GFPE Method

We consider a monopole source located above a finite impedance flat ground surface in an atmosphere with a non-constant sound speed profile and assume symmetry about the vertical axis z . We want to determine the pressure field $p(r, z)$, where r and z are the usual cylindrical coordinates, for the entire domain.

Removing the cylindrical spreading by introducing a variable $q = p \sqrt{r}$ and assuming valid the far-field approximation, the two-dimensional version of the Helmholtz equation becomes

$$\frac{\partial^2 q}{\partial r^2} + \frac{\partial^2 q}{\partial z^2} + k q = 0, \quad (1)$$

where $k(z) = \omega/c(z)$ is the wave number, ω is the angular frequency and $c(z)$ is the speed of sound. The Parabolic Equation (PE) method approximates equation (1) by a parabolic equation that is easier to solve numerically. There are a number of PE methods, but we chose to implement the Green Function PE method because of its computational speed. The derivation of the general GFPE method is based on the two-dimensional Kirchhoff-Helmholtz integral equation. Using a Green function formulation, it can be shown [1] that

$$\begin{aligned} \psi(r + \Delta r, z) = & e^{i \Delta r \frac{\delta k^2(z)}{2 k_a}} \left\{ \frac{1}{2 \pi} \int_{-\infty}^{+\infty} [\Psi(r, k_z) + R(k_z) \Psi(r, -k_z)] e^{i \Delta r \left(\sqrt{k_a^2 - k_z^2} - k_a \right)} e^{i k_z z} d k_z + \right. \\ & \left. + 2 i \beta \Psi(r, \beta) e^{-i \beta z} e^{i \Delta r \left(\sqrt{k_a^2 - k_z^2} - k_a \right)} \right\}, \quad (2) \end{aligned}$$

where

$$\Psi(r, k_z) = \int_0^{\infty} e^{i k_z z'} \psi(r, z') d z'. \quad (3)$$

Is the spatial Fourier Transform of the pressure field $\psi(r, z) = e^{-i k_a r} q(r, z)$. In equation (2), Δr is the horizontal spacing, k_a is a reference wave number and $\beta = k_0 / Z_g$. The plane wave reflection coefficient is $R(k_z) = (k_z Z_g - k_0) / (k_z Z_g + k_0)$, where Z_g is the ground impedance and k_0 is the wave number at zero height.

The atmospheric refraction is included in equation (2) by multiplying the solution of a homogeneous atmosphere by the exponential factor $\exp[i \Delta r \delta k^2(z) / (2 k_a)]$, where

$$k^2(z) = k_a^2 + \delta k^2(z). \quad (4)$$

As the GFPE method is a step by step extrapolation of the sound field $\psi(r + \Delta r, z)$, a two dimensional rectangular grid is used, where the two grid parameters (horizontal spacing Δr and vertical spacing Δz) are frequency dependent. The length of the numerical grid is defined as the number of horizontal steps necessary to reproduce the horizontal distance between the source and the receiver. Simultaneously, the grid is limited by the ground surface at $z = 0$ and by a top height $z_{top} = M \Delta z$, where M is a positive integer dependent on the source height. To prevent unrealistic wave reflections at the top of the numerical grid, an attenuation layer is located between $z = z_{abs}$ and $z = z_{top}$, where



its thickness typically varies between 50λ and 100λ , where λ is the average wavelength. This attenuation is obtained by adding an imaginary term to the wave number within the absorption layer, which is defined as

$$\alpha(z) = A \left(\frac{z - z_{abs}}{z_{top} - z_{abs}} \right)^2, \quad (5)$$

where A is a frequency dependent parameter.

To allow a correct comparison with benchmark results, we adopted a fourth order Gaussian starting field that is written as

$$q_0(0, z) = \sqrt{i k_a} (A_0 + A_2 k_a^2 z^2 + A_4 k_a^4 z^4 + A_6 k_a^6 z^6 + A_8 k_a^8 z^8) e^{\frac{k_a^2 z^2}{B}}. \quad (6)$$

where the coefficients A_i and B are determined by the order of the starting field [1]. The influence of a ground surface is included modifying equation (6) as

$$q(0, z) = q_0(z - z_s) + \frac{z_g - 1}{z_g + 1} q_0(z + z_s), \quad (7)$$

where z_s is the source height. To calculate the sound field it is necessary to compute multiple Fourier integrals in each extrapolation step. Consequently, each integral is approximated by a discrete sum named Discrete Fourier Transform (DFT).

3 The Ray Model

Outdoor sound propagation may be regarded as the propagation of multiple sound rays emanated from a source across the atmosphere; this approach is called geometrical acoustics. Consequently, the pressure amplitude at a specified location is given by the sum of the pressure amplitudes of each ray that passes through that position

$$p_c = \sum_{m=1}^{N_{rays}} A_m e^{i \phi_m}, \quad (8)$$

where A_m and ϕ_m are respectively the amplitude and phase of the m^{th} ray.

The computation of the total pressure at a specific receiver is correlated with the determination of all rays intersecting that location, thus being necessary to follow a procedure called ray tracing. The trajectory followed by a sound ray is obtained from the integration of Snell's law, which is defined as

$$\frac{\cos \gamma}{c} = \text{constant along a sound ray} \quad (9)$$

where γ is the angle of the ray's trajectory and $c = c(z)$ is the sound speed at the height where the calculation is done. Therefore, the trajectory of a sound ray in a homogeneous atmosphere is represented by a straight line while in a refracting atmosphere the sound rays are curved according to the speed gradient along the atmosphere.

3.1 Numerical formulation

As the process of ray tracing may become complex for low elevation angles and long range propagation in refracting atmospheres, we implemented a simplified version called two ray model where only two sound rays are considered, the direct ray and the reflected ray. The two ray model is only valid for large elevation angles, and consequently it can be verified that in its region of validity ray curvature is in practice negligible so an additional approximation is employed, where we consider both rays are modelled as straight rays.



Defining the source position as $(0, z_s)$ and the receiver location by (r, z) , the distance travelled by the direct ray is

$$R_1 = \sqrt{r^2 + (z - z_s)^2}. \quad (10)$$

On the other hand, the distance covered by the reflected ray may be calculated considering an imaginary source below the ground source, resulting in the following equation:

$$R_2 = \sqrt{r^2 + (z + z_s)^2}. \quad (11)$$

At last, the determination of the complex pressure amplitude follows the relation given by

$$p_c = S \frac{e^{i k R_1}}{R_1} + R_P S \frac{e^{i k R_2}}{R_2}, \quad (12)$$

where R_P is the plane wave reflection coefficient defined as

$$R_P = \frac{Z_g \cos \theta - 1}{Z_g \cos \theta + 1}. \quad (13)$$

4 The Hybrid Model

The GFPE propagation method is well suited for low elevation angles and it is valid for a wide variety of sound frequencies. It can be verified that the maximum elevation angle where accuracy can be attained is mainly due to the choice of an adequate starting field [2], while the other numerical variables have a lower influence on the region of validity. Therefore, it can be shown that a standard Gaussian field [3] provides accurate results up to an elevation angle of 35° whereas a higher-order starting field [1] as the one described in section 2 returns an accurate pressure field for a maximum angle of approximately 50° .

On the other hand, the simplified variant of the ray model implemented in this text is employed for high elevation angles, where the number of rays that reach the receiver's position is approximately two and the effects of atmospheric refraction are negligible. For that reason, the lower limit of the validity region of the two ray model is typically imposed at approximately 50° [4].

We developed a method that, while preserving a simple implementation in a programming language as the first, merges the sound pressure level obtained in the transition region (L_P) by employing a linear interpolation scheme between the results of the GFPE method ($L_{P,GFPE}$) and the ray model ($L_{P,Ray Model}$):

$$L_P = L_{P,GFPE} \frac{\gamma_{top} - \gamma}{\gamma_{top} - \gamma_{bottom}} + L_{P,Ray Model} \frac{\gamma - \gamma_{bottom}}{\gamma_{top} - \gamma_{bottom}}, \quad (14)$$

where γ is the elevation angle and γ_{bottom} and γ_{top} are respectively the lower and upper limits of the merging region. Equation (24) is only valid when the elevation angle γ is within the interval $\gamma_{bottom} \leq \gamma \leq \gamma_{top}$, otherwise we apply the following criterion

$$L_P = \begin{cases} L_{P,GFPE}, & \gamma < \gamma_{bottom} \\ L_{P,Ray Model}, & \gamma > \gamma_{top} \end{cases}. \quad (15)$$



5 Aircraft as a Noise Source

5.1.1 Aircraft Noise Power Spectrum

Noise certification plays an important role in an airplane design process. Therefore, several simulations and flight tests must be performed and the results must fulfil the requirements of the International Civil Aviation Organization [5] to guarantee the aircraft's airworthiness. The information regarding each airplane is condensed into one single public database called Aircraft Noise and Performance (ANP) database and three different quantities are tabulated: noise level, aircraft thrust setting and distance from the receiver (NPD, Noise-Power-Distance).

The ANP database can be used to retrieve the power spectrum of each aircraft by employing a reverse engineering method described in detail by Butikofer [6]. Using this process, we were able to obtain the power spectrum for different Airbus models, namely the A319/320/321, A330 and A340 families. The curve obtained from the spreadsheet relates the engine power spectrum with the 1/3-octave band centre frequencies.

As the determined spectra are only applicable for a limited number of thrust settings, in the computational application discussed in this text a linear interpolation algorithm for intermediate values was implemented.

5.1.2 Aircraft Noise Directivity

As aircraft are complex noise emitters, they cannot be modelled as a point source with an omnidirectional sound spreading. Therefore, the determination of the sound field must include additional correction factors that reflect the effects of lateral and longitudinal directivity. These effects are affected by the relative position between the source and the receiver and are governed by the angles θ and φ , where θ is the angle between the tangent to the flight path and the line connecting the aircraft to the observer and φ is the angle between the vertical plane and the plane that contains both the tangent to the flight path and the observer.

Lateral directivity is often called engine installation effect and it reflects the influence of the engine location and type on the overall directivity of the aircraft. This effect is directly related to the spherical angle φ . The SAE AIR 5662 [8] proposes two expressions that model the lateral effects of engine installation for fuselage mounted engines and wing mounted engines. For propeller driven aircraft there is no correction factor available.

Longitudinal directivity is mostly influenced by the engine characteristics as the bypass ratio and the type of fan installed. Ref. [6] provide the value of the correction factor $\Delta L_{longitudinal}$ as a function of the longitudinal angle θ for different classes of aircraft, namely jet powered aircraft (with four different generations of jet engines included), propeller driven vehicles and military airplanes.

6 Implementation and validation of the models

The implementations of the GFPE and Ray models were validated using the test cases published in [7]. The detailed results can be seen in [9].

The first stage of the implementation process of the hybrid model was the determination of suitable limits γ_{bottom} and γ_{top} to apply equation (5). This procedure consisted in the computation of the pressure field in a homogeneous atmosphere along four different downward travelling lines with elevation angles of 30°, 40°, 50° and 60°. The results obtained following this analysis suggest that limiting the merging zone between elevation angles of 40° and 50° is the more appropriate choice and therefore these limiting angles were adopted.

7 Results

To study the adequacy of the hybrid propagation model in an airport scenario, we simulated different aircraft trajectories based on the Airbus A320 at Lisbon airport. The parameters used in the simulations are listed in Tables 1 and 2.

Table 1 – Environmental parameters for the simulated airport scenarios.

Parameter	Value
Speed of Sound	340 m/s
Ambient Temperature	15 °C
Ground Surface	Airport Grass

Table 2 – Grid parameters for the simulated airport scenarios.

Parameter	Value
dr	10λ
dz	$\lambda/10$
z_{abs}	$2 z_{aircraft}$
$z_{top} - z_{abs}$	300λ
Starting field	Gaussian 4 th order

The first simulated trajectory was based on an ILS approach and the receiver was placed 2 km before the runway and aligned with the runway's centreline (see Figure 1). The results regarding the sound exposure level (SEL), which were compared with the experimental data published by Correia [10], are presented in Table 3. We may conclude that the numerical methods produce coherent results with the experimental data, as the relative deviation between both sets of values is acceptable.

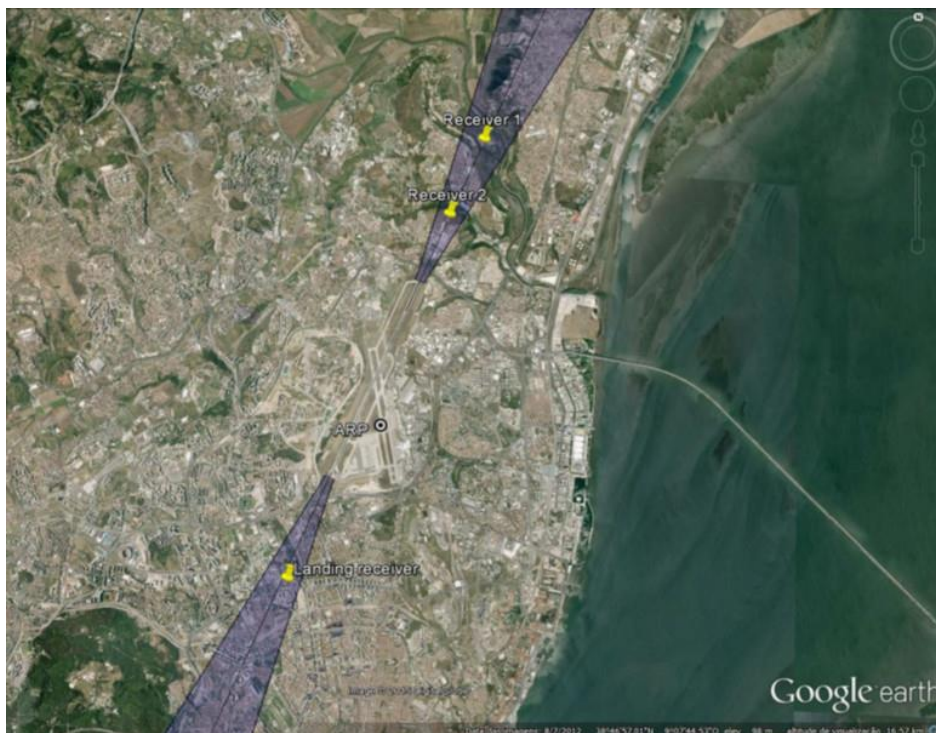


Figure 1 – Position of the receivers for the airport simulations.

Table 3 – SEL from numerical calculations and experimental measurements for the ILS approach.

Experimental	Numerical	Deviation
90.99 dB	88.3 dB	2.69 dB

We were also able to use the experimental data from two noise monitoring stations (located at Camarate and at the Airport) for a real departure procedure of a A320 from runway 03 at Lisbon Airport. The measured and calculated SEL, which are presented in Table 4, differ by 0.3 dB at Camarate station and 1.4 dB at the airport station. The maximum SPL differ by 0.6 dB at Camarate station and 4.0 dB at the airport stations. These results show that the model that was developed can be used with some confidence to predict noise level from aircraft in the vicinity of airports

Table 4 – SEL (dB) and L_{max} (dBA) for a real departure procedure of a A320 at Lisbon Airport.

Location ID	Location Description	SEL (dB)		L_{max} (dBA)	
		Experimental	Numerical	Experimental	Numerical
EMR 3	Camarate	89.8	89.5	81.3	80.7
EMR 7	Aeroporto	92.4	91.0	84.9	80.9

Another set of results obtained with the numerical program consisted of five noise reduction procedures for departing flights [11]. The procedures followed common guidelines and are characterized by three separate actions (see Table 5), which produce the trajectories shown in Figure 2.

Table 5 – Definition of the take-off stages (in feet AGL) for the departure trajectories.

	Case 1	Case 2	Case 3	Case 4	Case5
Thrust Reduction	800	800	1000	1500	1500
Flap Retraction	1500	800	1000	1500	3000
Acceleration to 250 kts	3000	3000	2500	1500	3000

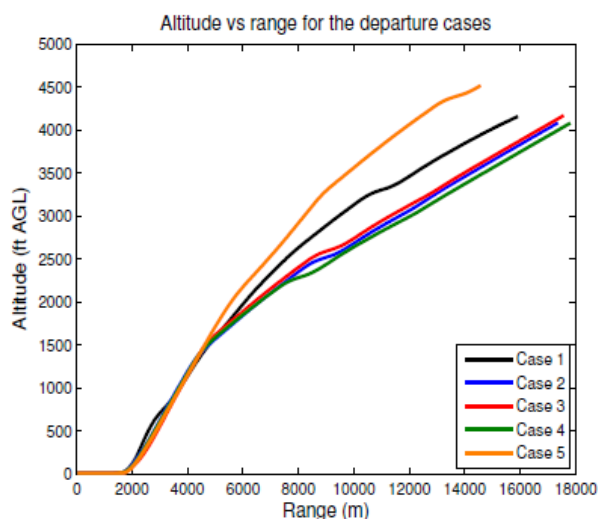


Figure 2 – Altitude as a function of distance to the start of take-off roll.

Table 6 presents the SEL results for two different receivers, the first one located at a distance of 6.5 km from the beginning of the take-off roll and aligned with the runway extended centreline and the other placed at a distance of 5 km. From the numerical results, we may conclude that noise abatement



trajectories are related to the region where sound levels are to be mitigated. Figure 3 shows the noise maps obtained with the numerical simulations for the 5 test cases.

The results suggest that, in order to minimize the impact of departing aircraft near the airport, engine thrust should be reduced to climb setting before reaching the observer. On the other hand, when reducing the noise indices in regions that are far from the runway, it can be verified that the aircraft should adopt a trajectory that increases the distance between the airplane and the receiver and consequently the power cutback action may be delayed to allow a longer climb segment at a higher climb gradient. In some situations, it may be unadvisable to delay the thrust reduction, which may result in overflying a noise monitoring terminal located closer to the runway end, at a higher thrust setting than if the thrust reduction was performed at a lower altitude

Table 6 – SEL (dB) for the reviewed departing procedures and for each receiver position.

	Case 1	Case 2	Case 3	Case 4	Case5
Receiver 1	85.7	86.2	86	86	85.5
Receiver 2	87.6	88.5	88.1	90.2	90.5

8 Conclusions

A noise prediction program oriented towards aviation noise in the vicinity of airports was developed using Matlab programming language. This computational tool includes physics-based atmospheric propagation methods and adopts empirical models that allow the definition of aircraft as complex noise sources.

The numerical schemes used to calculate sound propagation in the atmosphere were the Green's Function Parabolic Equation (GFPE) method and the two ray model. These methods were combined into a hybrid model in order to mitigate their limitations and maximize their potential.

The propagation methods were validated using benchmark test cases that are accepted as a standard in the verification of atmospheric sound propagation models. The adopted procedure involved three different stages, namely the validation of the GFPE method, the verification of the simplified ray model and the definition of the transition region. The similarity between the results from the implemented methods and the reference data allowed the validation of the numerical implementation process.

Finally, we discussed the application of the hybrid propagation model to an airport scenario by resorting to realistic flight conditions in two different stages. In the first part, we studied an approach simulation to Lisbon airport. The results obtained from the landing simulation were compared with published experimental results and the agreement between the numerical values and the experimental data confirmed the adequacy of the program to model real aircraft operations. Similar conclusion can be drawn from comparison of experimental and simulation results for a take-off from runway 03. In the last stage, we simulated a set of five noise reduction techniques for takeoffs that are typically used by airlines. The results obtained with these trajectories indicated that noise abatement procedures should be chosen according to the region where sound levels are to be minimized. Therefore, for receivers closer to the airport, thrust reduction should be accomplished before reaching the observer, while for regions far from the runway the initial climb segment, which is characterized by a steeper climb gradient, should be extended to allow the maximization of the distance between the aircraft and the observer.

Acknowledgements

This work was supported by FCT, through IDMEC, under LAETA, project UID/EMS/50022/2013.

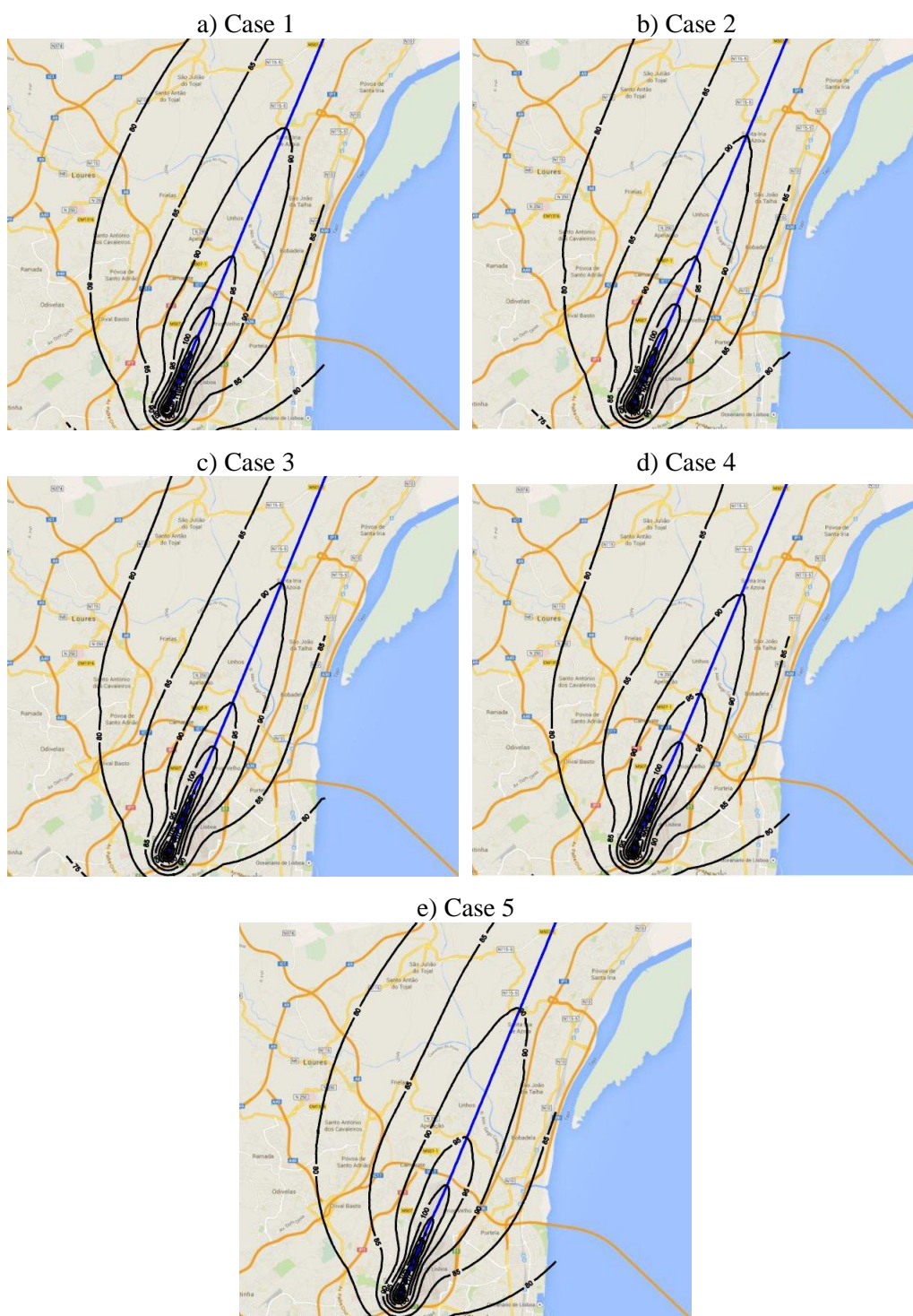


Figure 3 – Noise maps for the departure test cases, representing the aircraft's trajectory (blue line) and the SEL (in dB) contours (black lines).



References

- [1] Salomons, E. M. *Computational Atmospheric Acoustics*, Kluwer Academic Publishers, 2001
- [2] Cooper, J. L.; and Swanson, D. C. Parameter selection in the Green's function parabolic equation, *Applied Acoustics*, Vol 68, 2008, pp 390-402.
- [3] Gilbert, K. E.; Di, X. (1993). A fast Green's function method for one-way sound propagation in the atmosphere, *Journal of the Acoustical Society of America*, 94, 1993, pp. 2343–2352.
- [4] Boeker, E., and Rosenbaum, J. E. Intelligent switching between different noise propagation algorithms: analysis and sensitivity. *INTERNOISE 2012*, New York, August 19-22, 2014.
- [5] International Civil Aviation Organization. *Annex 16 to the convention on international civil aviation: Environmental Protection, Volume I: Aircraft Noise*, ICAO, 2005.
- [6] Butikofer, R. *Default aircraft source description and methods to assess source data*, Deliverable 10 of the IMAGINE project, 2006.
- [7] Attenborough, K. et al. Benchmark cases for outdoor sound propagation models, *Journal of the Acoustical Society of America*, Vol 97, 1995, pp. 173-191.
- [8] Society of Automotive Engineers, SAE Aerospace Information Report, *AIR 5662: Method for Predicting Lateral Attenuation of Airplane Noise*, SAE International, 2006.
- [9] Sousa, A. S. *Flight path optimization for noise reduction in the vicinity of airports*, M. Sc. Thesis, Instituto Superior Técnico, 2015.
- [10] Correia, G. S. D. *Previsão de níveis de ruído aeronáutico na vizinhança do Aeroporto de Lisboa*, M. Sc. Thesis, Instituto Superior Técnico, 2011.
- [11] International Civil Aviation Organization. *Review of noise abatement procedure research & development and implementation results*, ICAO, 2007.